

# Effect of surface tension on the mode selection of vertically excited surface waves in a circular cylindrical vessel\*

Jian Yong-Jun(菅永军)<sup>a)b)†</sup>, E Xue-Quan(鄂学全)<sup>b)</sup>,  
Zhang Jie(张杰)<sup>a)c)</sup>, and Meng Jun-Min(孟俊敏)<sup>a)c)</sup>

<sup>a)</sup>First Institute of Oceanography, State Oceanic Administration, Qingdao 266061, China

<sup>b)</sup>Institute of Mechanics, Chinese Academy of Sciences, Beijing 100080, China

<sup>c)</sup>Key Laboratory of Marine Science and Numerical Modelling, State Ocean Administration, Qingdao 266061, China

(Received 27 November 2003; revised manuscript received 27 July 2004)

Singular perturbation theory of two-time-scale expansions was developed in inviscid fluids to investigate pattern-forming, structure of the single surface standing wave, and its evolution with time in a circular cylindrical vessel subject to a vertical oscillation. A nonlinear slowly varying complex amplitude equation, which involves a cubic nonlinear term, an external excitation and the influence of surface tension, was derived from the potential flow equation. Surface tension was introduced by the boundary condition of the free surface in an ideal and incompressible fluid. The results show that when forced frequency is low, the effect of surface tension on the mode selection of surface waves is not important. However, when the forced frequency is high, the surface tension cannot be neglected. This manifests that the function of surface tension is to cause the free surface to return to its equilibrium configuration. In addition, the effect of surface tension seems to make the theoretical results much closer to experimental results.

**Keywords:** vertically forced oscillation, nonlinear amplitude equation, surface tension, surface wave modes

**PACC:** 0340G, 4754, 5235M, 9530L

## 1. Introduction

The classical hydrodynamics problem of vertically driven surface waves was first studied experimentally by Faraday.<sup>[1]</sup> He noticed that the resulting surface waves had a fundamental frequency of half the excitation frequency, i.e. the response was subharmonic. On the theoretical side, Ref.[2] studied the linear problem for ideal liquids enclosed in a container, vibrating sinusoidally in the vertical plane, and showed that the fluid dynamical equations can be reduced to a system of Mathieu equations, which allow harmonics as well as subharmonics. Faraday instability provides an excellent context containing the exploration of a variety of issues related to nonlinear pattern formation. A review of this subject was given in Ref.[3]. Many problems have been solved in inviscid fluids. However, until now, no reasonable nonlinear theory has been established for strongly damped surface waves.

Difficulties arise due to the interplay of intricate nonlinear boundary conditions at the free surface and the external excitation, which makes the problem non-autonomous.

Many flow patterns were observed in experiments<sup>[4–7]</sup> with one or two-frequency drive. These patterns included hexagons, triangles, twelvefold quasi-periodic pattern, two-dimensional quasi-crystal and supperlattice patterns, etc. Over the last two decades, Faraday instability has been extensively investigated for weakly viscous fluids in the confined and extended systems,<sup>[8–10]</sup> their secondary instabilities and transition to spatio-temporal chaos,<sup>[11,12]</sup> and turbulence.<sup>[13,14]</sup>

E *et al*<sup>[15–17]</sup> carried out the flow visualization and experimental studies on surface wave patterns in a circular cylindrical vessel using vertical external vibrations. They obtained very beautiful photographs of free surface patterns in a wide range of driving fre-

\*Project supported by the National Natural Science Foundation of China (Grant Nos 19772063, 19772068).

†Corresponding author: E-mail: jianyongjun@yahoo.com.cn

quency, and most of them had not been reported before.

Recently, Jian and E<sup>[18–20]</sup> proposed a mathematical formulation for both ideal and viscous fluids related to the flowing visualization in Refs.[15–17], from which the second-order free surface displacements and their contours were obtained by two-time-scale singular perturbation expansion. Although the numerical results of the contours of free surface waves agreed well with the experimental visualization, the forced frequency showed large differences. In addition, characteristics of the amplitude equation and stability analysis of the modified equation were studied respectively in Refs.[21] and [22].

In this paper, we study the Faraday resonance in an inviscid fluid in a circular cylindrical container by employing the two-time-scale perturbation expansion method and taking into account the effect of surface tension. A nonlinear slowly varying amplitude equation, similar to that derived by Jian and E,<sup>[18,19]</sup> is obtained from the Euler equation. The difference of the two amplitude equations is that the former includes the effect of surface tension. The coefficients of the amplitude equations with and without surface tension are compared with each other. It is shown that the theoretical forced frequency is much closer to the experimental results than that without surface tension effect.

## 2. Governing equation and boundary conditions for the vertically forced waves

We consider the surface waves excited by the vertical motion of a circular cylindrical basin filled with fluid. The physical model, all the parameters used and the choice of the coordinate system are the same as in Ref.[21].

It is assumed that the fluid is inviscid and incompressible, and the motion is irrotational. There must exist a velocity potential function  $\phi(r, \theta, z, t)$  satisfying the following governing equation:

$$\frac{\partial^2 \phi}{\partial r^2} + \frac{1}{r} \frac{\partial \phi}{\partial r} + \frac{1}{r^2} \frac{\partial^2 \phi}{\partial \theta^2} + \frac{\partial^2 \phi}{\partial z^2} = 0,$$

$$0 < r < R, \quad -h \leq z \leq \eta(r, \theta, t), \quad (1)$$

with the kinetic boundary condition being

$$\frac{\partial \phi}{\partial t} + \frac{1}{2} \left[ \left( \frac{\partial \phi}{\partial r} \right)^2 + \frac{1}{r^2} \left( \frac{\partial \phi}{\partial \theta} \right)^2 + \left( \frac{\partial \phi}{\partial z} \right)^2 \right] + (g - \ddot{z}_0)\eta - \frac{\Gamma}{\rho} \left( \frac{\partial^2 \eta}{\partial r^2} + \frac{1}{r} \frac{\partial \eta}{\partial r} + \frac{1}{r^2} \frac{\partial^2 \eta}{\partial \theta^2} \right) = 0,$$

$$z = \eta(r, \theta, t), \quad (2)$$

and the kinematic condition being

$$\frac{\partial \eta}{\partial t} + \frac{1}{r^2} \frac{\partial \phi}{\partial \theta} \frac{\partial \eta}{\partial \theta} + \frac{\partial \phi}{\partial r} \frac{\partial \eta}{\partial r} - \frac{\partial \phi}{\partial z} = 0,$$

$$z = \eta(r, \theta, t), \quad (3)$$

at the free surface. Here  $\eta(r, \theta, t)$  is the displacement of the surface from  $z=0$ ,  $R$  is the internal radius of the container, constants  $\Gamma$  and  $\rho$  denote the surface tension coefficient and the density of the fluid respectively. The effect of surface tension is introduced by the boundary condition of the free surface. In addition, since the influence of viscosity is ignored, the boundary conditions on the side-wall and at the bottom of the vessel become zero normal velocity for rigid container, namely

$$\frac{\partial \phi}{\partial r} = 0, \quad r = R, \quad (4)$$

$$\frac{\partial \phi}{\partial z} = 0, \quad z = -h. \quad (5)$$

Equations (1)–(5) establish the mathematical model that describes the nonlinear surface waves in an inviscid fluid under the effect of surface tension.

Firstly, taking the radius  $R$  of the vessel to be the length scale, and nondimensionalizing all the related independent and unknown variables, the following scalings are adopted:

$$z^* = z/R, \quad r^* = r/R, \quad \eta^* = \eta/R,$$

$$t^* = t/\sqrt{R/g}, \quad \phi^* = \phi / (R\sqrt{gR}),$$

$$\omega_0^* = \omega_0/\sqrt{g/R}, \quad \varepsilon^{*2} = 4A\omega_0^2/g,$$

$$A^* = A/R, \quad \Gamma^*/\rho^* = (gR^2) \Gamma/\rho. \quad (6)$$

Note that the asterisks denote dimensionless quantities and are subsequently dropped. The parameter  $\varepsilon^*$  quantifies the acceleration due to the vertical oscillation relative to gravity and is assumed to be much less than unity.

Substituting Eq.(6) into Eqs.(1)–(5), then expanding Eqs.(2) and (3) into Taylor series at  $z=0$  and neglecting the term  $O(\varepsilon^4)$ , we obtain the following nondimensional governing equation:

$$\frac{\partial^2 \phi}{\partial r^2} + \frac{1}{r} \frac{\partial \phi}{\partial r} + \frac{1}{r^2} \frac{\partial^2 \phi}{\partial \theta^2} + \frac{\partial^2 \phi}{\partial z^2} = 0,$$

$$0 < r < 1, \quad -h/R < z < 0, \quad (7)$$

with nonlinear free surface boundary conditions

$$\begin{aligned} & \frac{\partial \phi}{\partial t} + \frac{1}{2} \left[ \left( \frac{\partial \phi}{\partial r} \right)^2 + \frac{1}{r^2} \left( \frac{\partial \phi}{\partial \theta} \right)^2 + \left( \frac{\partial \phi}{\partial z} \right)^2 \right] \\ & + [1 + \varepsilon^2 \cos(2\omega_0 t)] \eta \\ & - \frac{\Gamma}{\rho} \left( \frac{\partial^2 \eta}{\partial r^2} + \frac{1}{r} \frac{\partial \eta}{\partial r} + \frac{1}{r^2} \frac{\partial^2 \eta}{\partial \theta^2} \right) + \frac{\partial^2 \phi}{\partial t \partial z} \eta \\ & + \left( \frac{\partial \phi}{\partial r} \frac{\partial^2 \phi}{\partial r \partial z} + \frac{1}{r^2} \frac{\partial \phi}{\partial \theta} \frac{\partial^2 \phi}{\partial \theta \partial z} + \frac{\partial \phi}{\partial z} \frac{\partial^2 \phi}{\partial z^2} \right) \eta \\ & + \frac{1}{2} \frac{\partial^3 \phi}{\partial t \partial z^2} \eta^2 = 0, \quad z = 0; \quad (8) \\ & \frac{\partial \eta}{\partial t} - \frac{\partial \phi}{\partial z} + \frac{\partial \phi}{\partial r} \frac{\partial \eta}{\partial r} + \frac{1}{r^2} \frac{\partial \phi}{\partial \theta} \frac{\partial \eta}{\partial \theta} \\ & - \frac{\partial^2 \phi}{\partial z^2} \eta + \frac{\partial^2 \phi}{\partial r \partial z} \eta \frac{\partial \eta}{\partial r} + \frac{1}{r^2} \frac{\partial^2 \phi}{\partial \theta \partial z} \eta \frac{\partial \eta}{\partial \theta} \\ & - \frac{1}{2} \frac{\partial^3 \phi}{\partial z^3} \eta^2 = 0, \quad z = 0; \quad (9) \end{aligned}$$

and the boundary conditions on side-wall and at the bottom are

$$\frac{\partial \phi}{\partial r} = 0, \quad r = 1; \quad (10)$$

$$\frac{\partial \phi}{\partial z} = 0, \quad z = -h/R. \quad (11)$$

In order to solve Eqs.(7)–(11) by the two-time-scale perturbation expansion, a slowly varying time scale  $\tau$  is introduced. Letting  $\tau = \varepsilon^2 t$ , we have

$$\partial/\partial t = \partial/\partial t + \varepsilon^2 \partial/\partial \tau + \dots, \quad (12)$$

where  $\partial/\partial t$  denotes the derivative with respect to time  $t$ . The slowly varying time scale is necessary since we are going to perform our perturbation expansion up to  $O(\varepsilon^3)$ , in which the influence of external excitation can be incorporated and the amplitude equation of the surface wave can be determined. To seek the solutions to  $\phi(r, \theta, z, t)$  and  $\eta(r, \theta, t)$ , we expand them into power series of  $\varepsilon$

$$\begin{aligned} \phi(r, \theta, z, t, \tau) &= \varepsilon \phi_1 + \varepsilon^2 \phi_2 + \varepsilon^3 \phi_3 + \dots \\ \eta(r, \theta, t, \tau) &= \varepsilon \eta_1 + \varepsilon^2 \eta_2 + \varepsilon^3 \eta_3 + \dots \quad (13) \end{aligned}$$

Substituting Eqs.(12) and (13) into nondimensional Eqs.(7)–(11), we can give the approximate equations by comparing the coefficients of the small parameter  $\varepsilon^i$  on the two sides of the equations.

### 3. The approximate solution in each order

The method used here is similar to that in Refs.[18–20], and the only difference between them is

that here the influence of surface tension is taken into account under the free surface boundary condition. Due to the complexity of mathematical formulation, the detailed derivation will be presented in another paper, and only the important results are given as follows.

The first-order velocity potential  $\phi_1(r, \theta, z, t, \tau)$  and free surface displacement  $\eta_1(r, \theta, t, \tau)$  can be expressed as

$$\begin{aligned} \phi_1 &= J_m(\lambda r) \cosh[\lambda(z + h/R)] \\ &\quad \times [p(\tau) e^{i\Omega t} + \bar{p}(\tau) e^{-i\Omega t}] \cos m\theta, \quad (14) \end{aligned}$$

$$\begin{aligned} \eta_1 &= \frac{\lambda}{i\Omega} J_m(\lambda r) \sinh(\lambda h/R) \\ &\quad \times [p(\tau) e^{i\Omega t} - \bar{p}(\tau) e^{-i\Omega t}] \cos m\theta. \quad (15) \end{aligned}$$

The dispersion relation is

$$\Omega^2 = \lambda_{mn} \tanh(\lambda_{mn} h/R) \left( 1 + \frac{\Gamma}{\rho} \lambda_{mn}^2 \right) = \Omega_{mn}^2, \quad (16)$$

where  $\lambda = \lambda_{mn}$  are the positive real roots of  $dJ_m(\lambda_{mn} r)/dr |_{r=1}=0$ ,  $J_m(r)$  is the first kind  $m$ th-order *Bessel* function,  $p(\tau)$  is called the slowly varying complex amplitude and  $\bar{p}(\tau)$  denotes the complex conjugate of  $p(\tau)$ ,  $\Omega$  is the natural frequency of the surface wave.

The second-order velocity potential  $\phi_2(r, \theta, z, t, \tau)$  and free surface displacement  $\eta_2(r, \theta, t, \tau)$  can be expressed as

$$\begin{aligned} \phi_2(r, \theta, z, t, \tau) &= [X_1(r, z) + X_2(r, z) \cos(2m\theta)] \\ &\quad \times (p^2(\tau) e^{2i\Omega t} - \bar{p}^2(\tau) e^{-2i\Omega t}), \quad (17) \end{aligned}$$

$$\begin{aligned} \eta_2(r, \theta, t, \tau) &= [Y_1(r) + Y_2(r) \cos(2m\theta)] \\ &\quad \times (p^2(\tau) e^{2i\Omega t} + \bar{p}^2(\tau) e^{-2i\Omega t}), \quad (18) \end{aligned}$$

where  $Y_1(r)$  and  $Y_2(r)$  are functions of variable  $r$ , and  $X_1(r, z)$  and  $X_2(r, z)$  are functions of variables  $r$  and  $z$ . The detailed expressions of them are ignored in this paper.

Since the third-order problem is inhomogeneous and the first-order homogeneous problem has a non-trivial solution, it is necessary to apply a solvability condition to ensure the solution to the third-order problem. Finally, the solvability condition is obtained as

$$i \frac{dp(\tau)}{d\tau} = M_1 p^2(\tau) \bar{p}(\tau) + M_2 e^{2i\sigma\tau} \bar{p}(\tau), \quad (19)$$

where  $i$  is the unit of imaginary number,  $M_1$  and  $M_2$  are constants. Although the form of Eq.(19) is equivalent to Eq.(65) in Refs.[18, 19], the former includes

the effect of surface tension. In addition, we assume that the frequency  $\Omega$  of the free surface wave is close to one half of the forced oscillation frequency  $\omega_0$ , and let  $\omega_0 - \Omega = \varepsilon^2 \sigma$ .

Similarly, defining  $p_1(\tau)$  and  $p_2(\tau)$  as the real and imaginary parts of  $p(\tau)$ , and dividing Eq.(19) into real and imaginary parts, we have the following non-linear ordinary differential equation group:

$$\begin{aligned} \frac{dp_1(\tau)}{d\tau} = & M_1 p_2(\tau) [p_1^2(\tau) + p_2^2(\tau)] \\ & + M_2 [p_1(\tau) \sin(2\sigma\tau) - p_2(\tau) \cos(2\sigma\tau)], \end{aligned} \quad (20)$$

$$\begin{aligned} \frac{dp_2(\tau)}{d\tau} = & -M_1 p_1(\tau) [p_1^2(\tau) + p_2^2(\tau)] \\ & - M_2 [p_1(\tau) \cos(2\sigma\tau) + p_2(\tau) \sin(2\sigma\tau)]. \end{aligned} \quad (21)$$

The displacement of the free surface can be expressed as follows:

$$\eta(r, \theta, t, \tau) = \varepsilon \eta_1 + \varepsilon^2 \eta_2, \quad (22)$$

where the first-order and second-order free surface displacements  $\eta_1(r, \theta, t, \tau)$  and  $\eta_2(r, \theta, t, \tau)$  are given by Eqs.(15) and (18) respectively.

## 4. The computational results

### 4.1. The influence of the surface tension on mode selection

In order to demonstrate the influence of surface tension on the natural frequency and mode selection, the variation of the dimensional natural frequency with the wave number is illustrated in Fig.1, which is obtained by using the dispersive relation (16). The selection of parameters is similar to that in experiments.<sup>[15-17]</sup>

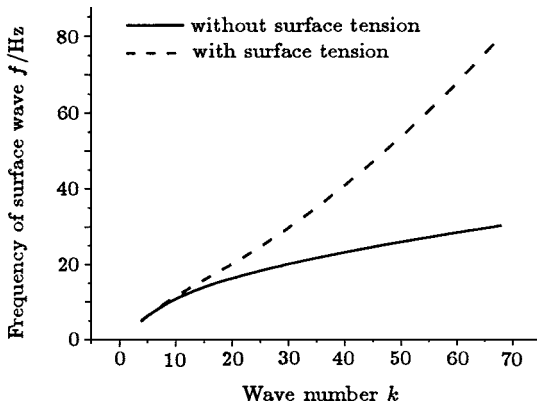


Fig.1. Variation of dimensional natural frequency with wave number (depth of fluid  $h=1.0\text{cm}$ , radius of the vessel  $R=7.5\text{cm}$ , surface tension coefficient  $\Gamma=0.0727\text{N/m}$ , density of fluid  $\rho=10^3\text{kg/m}^3$ ).

It can be seen from Fig.1 that the frequency of the surface waves increases with the wave number no matter whether the surface tension is included or not. When the forced frequency is low, the effect of surface tension on mode selection can be ignored. However, when the forced frequency is high, the effect of surface tension is significant.

Figure 2 shows how the relative increment, defined as the ratio of the frequency difference between frequencies with and without surface tension to the frequency without surface tension, varies with the forced frequency without surface tension.

It is clearly seen from Fig.2 that the influence of the surface tension cannot be ignored when the forced frequency is larger than 13Hz, and it needs additionally more than 10% forced frequency to attain the same surface mode when the surface tension is included.

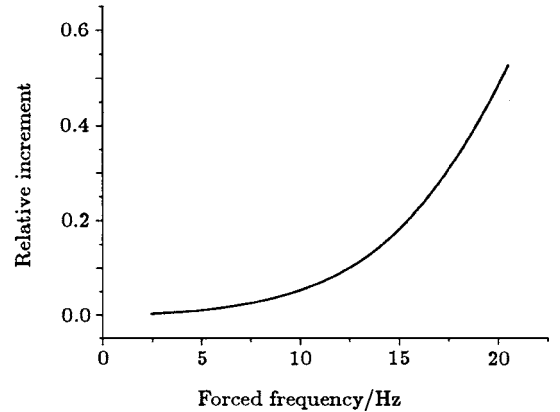


Fig.2. Variation of the relative increment with forced frequency without taking surface tension into account (depth of fluid  $h=1.0\text{cm}$ , radius of the vessel  $R=7.5\text{cm}$ , surface tension coefficient  $\Gamma=0.0727\text{N/m}$ , density of fluid  $\rho=10^3\text{kg/m}^3$ ).

### 4.2. The comparison of the coefficients of the amplitude equation

We have pointed out that the coefficients of Eq.(19) include the effect of the surface tension. In this section, we give the computational results to describe the variation of the coefficients  $\sigma$ ,  $M_1$  and  $M_2$  of Eq.(19) with the forced frequency in Figs.3(a), 3(b), and 3(c) respectively under the conditions with and without surface tension taken into account.

It can be seen from Fig.3(a) that the coefficient of the frequency difference  $\sigma$  changes considerably no matter whether the surface tension is incorporated or not when the wave number is low. This reflects that

the discrepancy between the natural frequency and the one half of the forced frequency is large. With the increase of the forced frequency, the number of optional patterns corresponding to the same wave number increases at a fixed forced frequency. Thus the discrepancy between the natural frequency and the forced frequency decreases. In this case, the frequency difference coefficient  $\sigma$  decreases gradually.

In Fig.3(b), the nonlinear coefficient  $M_1$  changes more sharply under the condition with the surface tension than that without surface tension. From the point of view of equilibrium, the value of solution  $p(\tau)$  to Eq.(19) with the surface tension is smaller than that

without surface tension, and the cubic of  $p(\tau)$  is much smaller. In order to keep equilibrium in Eq.(19), the nonlinear coefficient  $M_1$  must be large enough when the surface tension is taken into account. This means that surface tension has the property of keeping the system stable.

Figure 3(c) shows that the external forced coefficient  $M_2$  increases with the forced frequency, with or without surface tension (we only consider the absolute value of  $M_2$  which is multiplied by  $\varepsilon^2$ ). We can see that  $M_2$  changes slowly when the surface tension is taken into account. This also indicates that surface tension has the function of keeping the system stable.

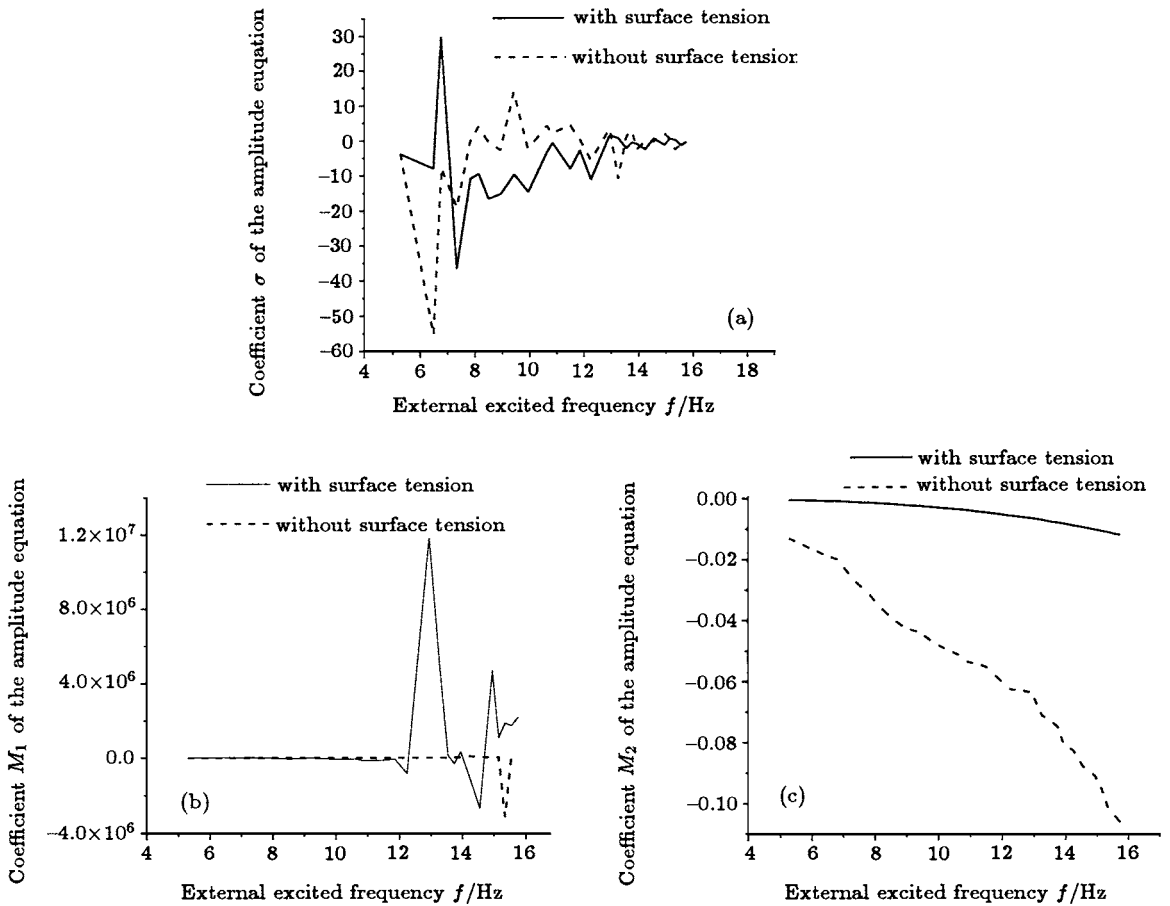


**Fig.3.** Variation of the coefficients in amplitude equation (19) with the forced frequency (forced amplitude  $A=11.4\mu\text{m}$ , other parameters are same as in Fig.2). (a) Variation of the frequency difference coefficient  $\sigma$  with forced frequency; (b) Variation of the nonlinear coefficient  $M_1$  with forced frequency; (c) Variation of the external excited coefficient  $M_2$  with forced frequency.

### 4.3. The relation between the surface wave mode and the depth of fluid

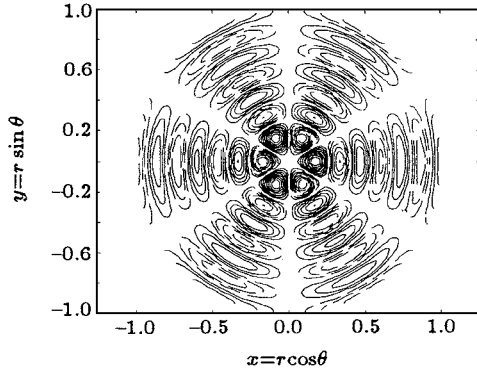
The surface wave modes are different for different depths of fluids at the same forced frequency and forced amplitude. When the forced amplitude is  $11.4\mu\text{m}$  and forced frequency is  $15.5\text{Hz}$ , the contours  $(4(a_1), 4(b_1), 4(c_1))$  and corresponding three-

dimensional surface figures  $(4(a_2), 4(b_2), 4(c_2))$  of the free surface displacements, which are determined by the solutions to Eqs.(20)–(22), are plotted in Fig.4 with the depths being 0.3, 0.5 and 0.8cm respectively.

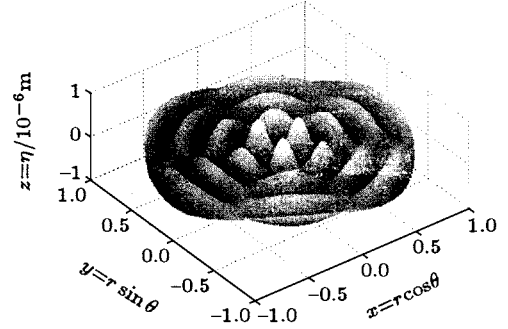
In Fig.4, the meaning of the solid or dashed lines of the contours and the parametrical couple of  $(m, n)$  are the same as those in Refs.[18–20]. We can see from Fig.4 that the modes of surface wave become simpler

with the increase of the depth of fluid. The reason is that the wave number decreases with the increase of

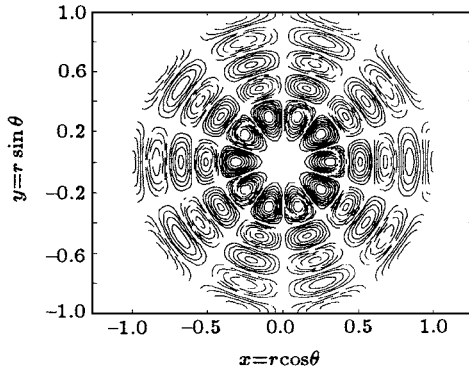
the depth of fluid when the natural frequency is fixed, which can be seen from the dispersive relation (16).



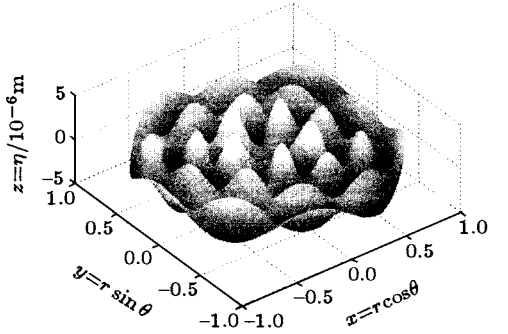
(a<sub>1</sub>) contour of (3, 7) mode ( $h=0.30\text{cm}$ ).



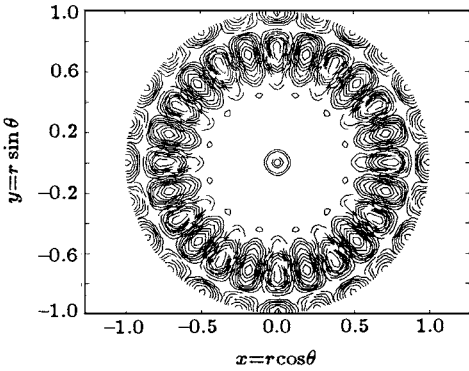
(a<sub>2</sub>) three-dimensional surface figure of (3, 7) mode.



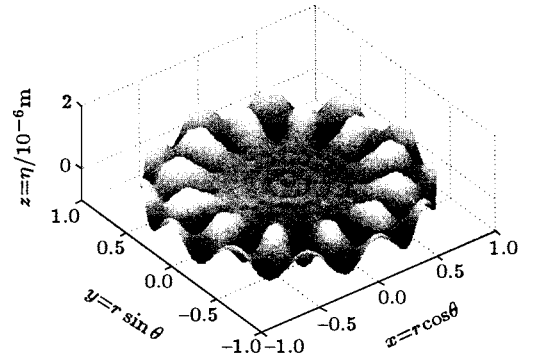
(b<sub>1</sub>) contour of (5, 5) mode ( $h=0.50\text{cm}$ ).



(b<sub>2</sub>) three-dimensional surface figure of (5, 5) mode.



(c<sub>1</sub>) contour of (12, 2) mode ( $h=0.80\text{cm}$ ).



(c<sub>2</sub>) three-dimensional surface figure of (12, 2) mode.

Fig.4. Variation of the mode of surface wave with the depth of fluid (forced frequency  $f=15.5\text{Hz}$ , forced amplitude  $A=11.4\mu\text{m}$ , the radius of vessel is  $R=7.5\text{cm}$ ).

## 5. Comparisons with experiment

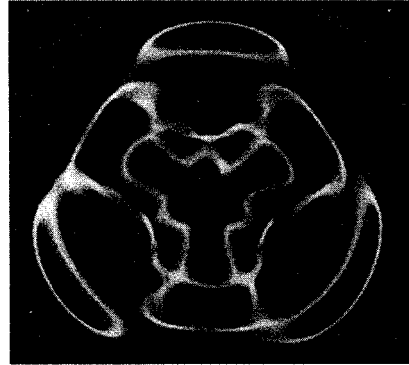
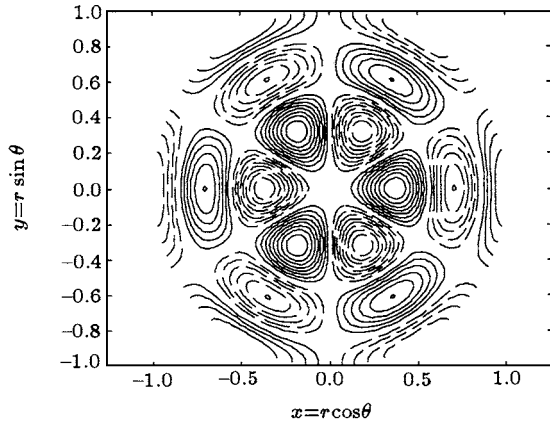
The theoretical contours were compared with those obtained from Refs.[15–17] in Fig.5 at different forcing frequencies. When the effect of surface tension is taken into account, the theoretical results are much closer to experimental results. In Fig.5, left figures are the computational results, and right ones are the experimental contours of flow patterns.

In order to explain the influence of surface tension clearly, we compared the results of having surface tension with those of no surface tension in Table 1. It can be seen from Table 1 and Fig.5 that the influence of surface tension becomes more and more important with the increase of wave number. However, the discrepancy of forced frequency is still very large. The reason is possibly due to the influence of contact line, the mode competition and the viscosity of the fluid,

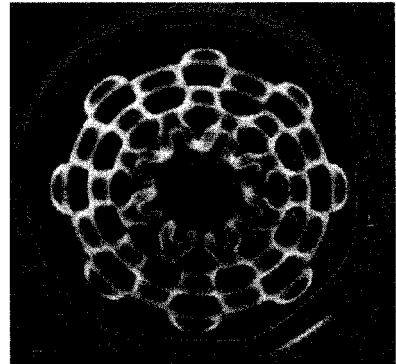
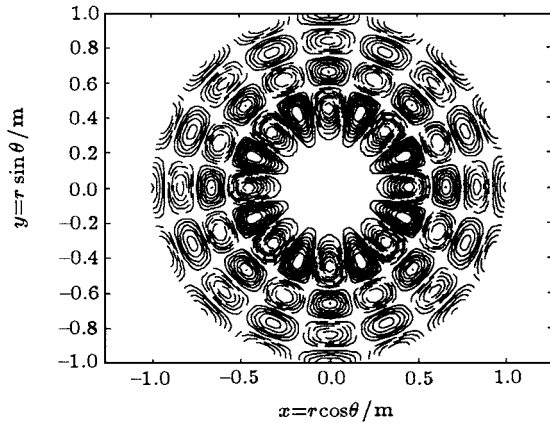
etc. The influence of the weak viscosity on the mode selection has been discussed in Ref.[20].

**Table 1.** Comparison of the forced frequency with surface tension and without surface tension for different patterns appeared both in theory and experiment.

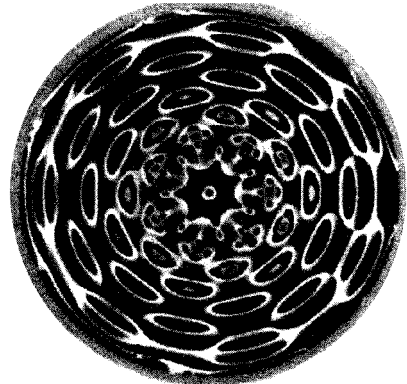
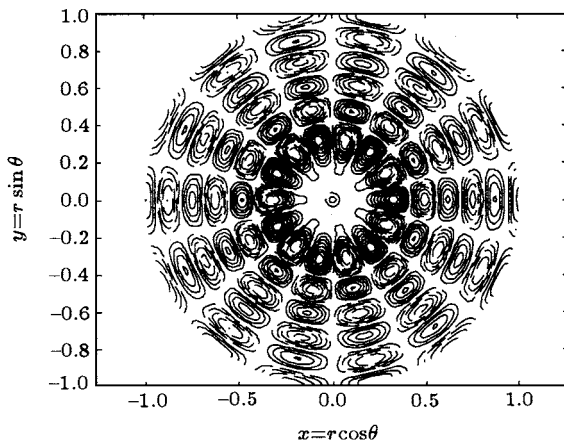
Pattern ( $m, n$ )	Wave number	Forced frequency without surface tension/Hz	Forced frequency with surface tension/Hz	increment/Hz
(3, 3)	11.346	11.68	12.63	0.95
(8, 4)	21.229	16.71	21.10	4.39
(7, 6)	26.545	18.74	26.02	7.28



(a) (3, 3) mode (left) forced frequency  $f=12.63\text{Hz}$ , (right) forced frequency  $f=20\text{Hz}$ .



(b) (8, 4) mode (left) forced frequency  $f=21.10\text{Hz}$ , (right) forced frequency  $f=50\text{Hz}$ .



(c) (7, 6) mode (left) forced frequency  $f=26.02\text{Hz}$ , (right) forced frequency  $f=52\text{Hz}$ .

**Fig.5.** Comparison of theoretical contours of surface wave mode with those of experiment (depth of fluid  $h=1.0\text{cm}$ , radius of the vessel  $R=7.5\text{cm}$ , the forcing amplitude  $A=11.4\mu\text{m}$ ).

## 6. Conclusions

From the above analysis, the following results can be obtained:

A. The nonlinear amplitude equations (20)–(21) and free surface displacement (22) can be used to correctly describe the surface wave motion in a vertically excited vessel.

B. When the wave number is small, the influence of the surface tension on pattern selection is insignificant. However, when the wave number is large, the effect of the surface tension is important.

C. For prescribed forced frequency and amplitude,

the patterns of surface waves become simple with increase of the depth of the fluid.

D. The surface tension has the function to cause the agitated free surface to return to equilibrium configuration. That is to say, when the surface tension is taken into account, it needs an higher forced frequency to produce the same flow pattern.

## Acknowledgement

The authors are grateful to Professor Zhou Xi-anchu for discussion on the aspects of mathematical treatment, and Dr Bai Wei for his assistance with the numerical work.

## References

- 
- [1] Faraday M 1831 *Phil Trans R. Soc. Lond.* **121** 319
  - [2] Benjamin T B and Ursell F 1954 *Proc R. Soc. Lond.* **255** 505
  - [3] Miles J W and Henderson D 1990 *Ann. Rev. Fluid Mech.* **22** 143
  - [4] Christiansen *et al* 1992 *Phys. Rev. Lett.* **68** 2157
  - [5] Müller H W 1993 *Phys. Rev. Lett.* **71** 3287
  - [6] Edwards W S and Fauve S 1994 *J. Fluid Mech.* **278** 123
  - [7] Kudrolli *et al* 1998 *Physica D* **123** 99
  - [8] Wu J *et al* 1984 *Phys. Rev. Lett.* **52** 1421
  - [9] Zhang W and Viñals J 1997 *J. Fluid Mech.* **336** 301
  - [10] Chen P and Viñals J 1997 *Phys. Rev. Lett.* **14** 2670
  - [11] Ciliberto S and Gollub J P 1985 *J. Fluid Mech.* **158** 381
  - [12] Kudrolli and Gollub J P 1996 *Physica D* **97** 113
  - [13] Pushkarev A N and Zakharov V E 1996 *Phys. Rev. Lett.* **76** 3320
  - [14] Schröder E *et al* 1996 *Phys. Rev. Lett.* **76** 4717
  - [15] E X Q and Gao Y X 1996 *Commun. Nonlinear Sci. Numer. Simul.* **1** 1
  - [16] E X Q and Gao Y X 1996 *Proceedings of the Fourth Asian Symposium on Visualization Beijing* 653
  - [17] Gao Y X and E X Q 1998 *Exp. Mech.* **13** 326 (in Chinese)
  - [18] Jian Y J *et al* 2003 *Appl. Math. Mech.* **24** 1194 (English Edition)
  - [19] Jian Y J and E X Q 2003 *J. Hydrodynam.* **18** 135 (in Chinese)
  - [20] Jian Y J and E X Q 2004 *Chin. Phys.* **13** 1191
  - [21] Jian Y J *et al.* 2004 *Chin. Phys.* **13** 1623
  - [22] Jian Y J and E X Q 2004 *Chin. Phys.* **13** 1631